REVIEW OF NEUTRINO EXPERIMENTS

D.H. Perkins

Department of Nuclear Physics,
University of Oxford, Oxford, England.

INTRODUCTION

This review will cover the following topics in charged current neutrino interactions:-

(1) Elastic processes, $\nu n \to \mu^- p$ and $\nu p \to \mu^+ n$

(2) 1π, 2π and 3π production

(3) Inclusive cross-sections

(4) Scaling, x and y distributions, sumrules in deep inelastic scattering

(5) Strange particle production

(6) Anomalies in x, y distributions, violations of charge symmetry and sumrules.

In addition I shall discuss:-

(7) Evidence for and against existence of heavy long-lived neutral leptons, suggested by the Kolar Gold Field cosmic neutrino experiment.

I shall NOT discuss dimuons, which are covered in the papers of B. Barish and C. Rubbia, and to which I can add nothing useful; or neutral currents, which are fully described in the papers of J. Morfin and L. Wolfenstein.

I THE ELASTIC REACTIONS $\nu + n \to \mu^- + p$, $\bar{\nu} + p \to \mu^+ + n$

The most recent results on the determination of the weak nucleon form-factors have been obtained by the ANL-Purdue collaboration. A total of 396 examples were observed of the reaction $\nu d \to \mu^- p p_s$ where p_s is the spectator proton. The technical details of the experiment, carried out in the ANL 12' chamber with deuterium filling, have been described previously[1].

Making the traditional assumptions - time reversal invariance, first-class currents, neglect of the induced pseudoscalar term - the cross-sections determine the vector and axial vector form-factors, parametrized via the dipole fit

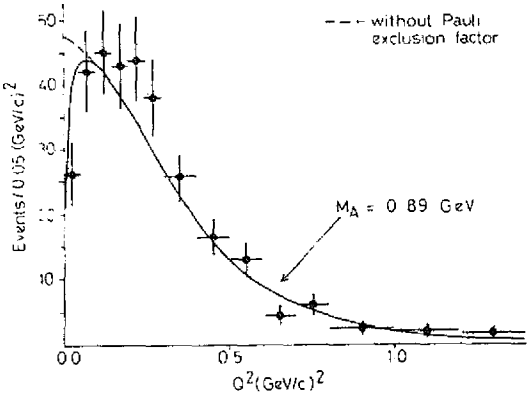

Fig. 1 q^2 distribution observed for the elastic reaction $\nu + n \rightarrow \mu^- + p$ in deuterium, by ANL-Purdue groups.

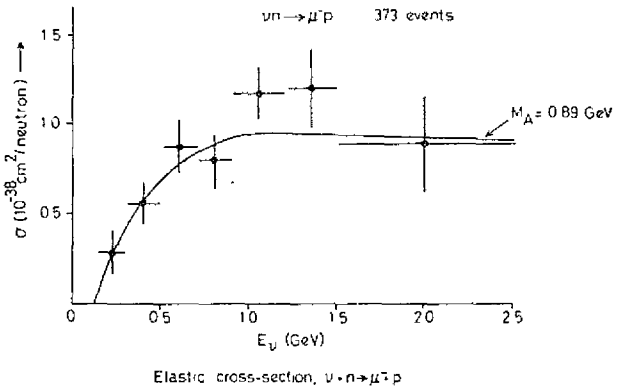

Fig. 2 Elastic cross-section for $\nu + n \rightarrow \mu^- + p$ as a function of energy.

$$G_{V,A} = (1 + q^2/M_{V,A})^{-2}$$

with masses M_V and M_A respectively. If the extended CVC (isotriplet current) hypothesis is assumed, M_V = 0.84 GeV from electron scattering. Two values of M_A are obtained, from $d\sigma/dq^2$ and $\sigma(E)$ respectively (see Figs. 1 and 2):-

q^2 shape: $M_A = 0.84 \pm 0.11$ GeV

$\sigma(E)$: $M_A = 0.98 \pm 0.13$ GeV

The second value depends directly on the neutrino flux calibration and the error includes the flux uncertainty, whereas the first is essentially flux-independent. If the q^2 and cross-section data are combined, one obtains

$$M_A = 0.89 \pm 0.08 \text{ GeV} \qquad (1)$$

If the CVC hypothesis is relaxed, both M_V and M_A are determined independently to be

$$M_V = 0.92 \pm \begin{matrix} 0.05 \\ 0.11 \end{matrix} \quad \text{GeV}$$

$$M_A = 0.75 \pm \begin{matrix} 0.21 \\ 0.10 \end{matrix} \quad \text{GeV}$$

Data on the antineutrino process, $\bar{\nu} + p \rightarrow \mu^+ + n$, is at present available only from the CERN Gargamelle experiment in freon[2]. The q^2 distributions, the ν and $\bar{\nu}$ cross-sections, and the ν, $\bar{\nu}$ cross-section difference all yield values of M_A consistent with (1). However these results are intrinsically less reliable than those from deuterium because of more severe nuclear corrections. Fig. 3 shows both the ANL and CERN cross-sections, quoted per nucleon of freon (CF_3Br). They are consistent with the expected dependence for M_A = 0.9 GeV

Finally it should be mentioned that all the neutrino experiments to date yield values of M_A somewhat below 1 GeV. This is to be contrasted with those extracted from analysis of pion electroproduction, using PCAC and soft-pion techniques, which are systematically above 1 GeV (see the report of G. Wolf at this conference.)

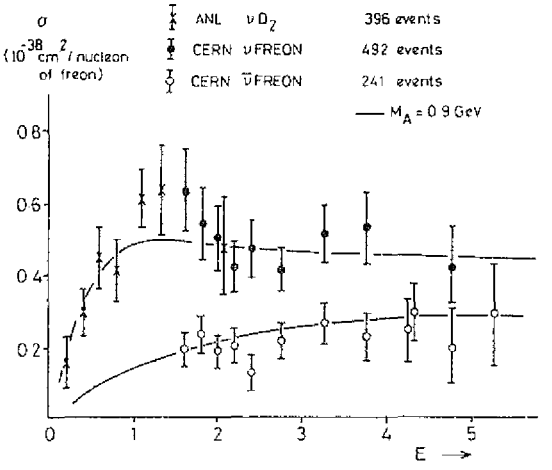

Fig. 3 Elastic cross-section on nucleons as a function of energy, calculated per nucleon of freon (CF_3Br), as measured for neutrinos CERN, ANL) and antineutrinos (CERN).

II WEAK PION PRODUCTION

IIa Single Pion Production

The ANL-Purdue group have continued their study of single pion production by neutrinos in hydrogen and deuterium.[3] The reactions studied were

$$\nu p \to \mu^- p \pi^+ \qquad (2a)$$

$$\nu d \to \mu^- p \pi^+ (n_s) \qquad (2b)$$

$$\nu d \to \mu^- n \pi^+ (p_s) \qquad (2c)$$

$$\nu d \to \mu^- p \pi^\circ (p_s) \qquad (2d)$$

The first two reactions involve a pure I = $^3/2$ final hadron state. (2a) provides a 3C kinematic fit, and (2b) is constrained if one sets reasonable upper limits on the spectator neutron momentum; the cut p < 50 MeV/c on each of the x, y, z momentum components was employed, removing 9 ± 2% of genuine events.

In contrast (2c) and (2d) involve both I = $\frac{1}{2}$ and I = $^3/2$ final states, and are not constrained because of the missing neutral. They are detected by means of the missing momentum transverse to the beam direction. The events selected however contain considerable background, arising from incoming pions, from elastic events, from examples of reaction (2b), and from 2π production. Various transverse momentum cuts and reconstructed neutrino and neutron energy cuts are applied, essentially removing all the background. The loss of genuine events can be assessed using the $\mu^- p \pi^+$ sample treated in similar fashion. At high energy, 2π background becomes large and the cross-sections are not quoted above 1.5 GeV.

Fig. 4 shows the pion nucleon mass spectra obtained for the 4 reactions in equation (2). Both reactions (2a) and (2b) are included in Fig. 4(a); the neutron spectator events satisfying the selection criteria for reactions (2c) and (2d) are shown shaded. Fig. 4(a) shows a strong Δ signal, whereas the Δ does not dominate in the $n\pi^+$ and $p\pi^\circ$ reactions.

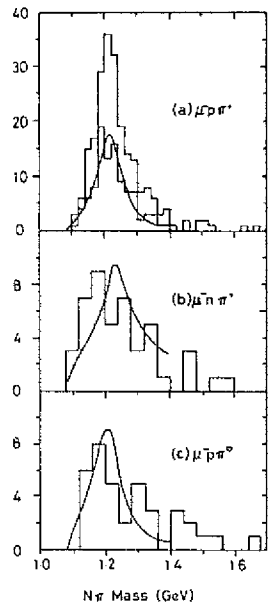

Fig. 4 Pion-nucleon mass spectrum observed in weak pion production. The curves shown are those computed from the Adler model. The shaded area in (a) corresponds to events in deuterium with a spectator neutron.

The amplitude of the different reactions can be written:-

$$A(\pi^+p) = A_3 - B_3/\sqrt{5}$$
$$A(\pi^+n) = A_3/3 + 2A_1/3 + B_3/\sqrt{5} \qquad (3)$$
$$A(\pi^\circ p) = \sqrt{2}A_3/3 - \sqrt{2}A_1/3 + \sqrt{2}B_3/\sqrt{5}$$

where A_1 and A_3 are isovector exchange amplitudes feeding $I = \frac{1}{2}$ and $I = 3/2$ final states, and B_3 is a possible isotensor exchange amplitude, assumed to feed $I = 3/2$ states only. The analysis of event rates leads to the following results:-

(i) The triangle inequalities implied by equation (3) are found to be satisfied if

$$-0.52 \pm 0.11 \lesssim B_3/A_3 \lesssim 0.23 \pm 0.07$$

consistent with no isotensor exchange.

(ii) Assuming $B_3 = 0$, and for $M_{\pi N} < 1.4$ GeV, the ratio and relative phase of the isovector amplitudes are

$$|A_1|/|A_3| = 0.78 \pm 0.15$$

$$\phi = 92 \pm 10^\circ,$$

implying a large non-resonant $I = \frac{1}{2}$ πN background in the $I = 3/2$ resonance (Δ) region. The magnitude of the $I = \frac{1}{2}$ amplitude is in fair agreement with the dispersion calculations of Adler[4]. The mass distributions according to the Adler model are shown in Fig. 4. Quantitatively, the values of A_1 and A_3 can also be specified in terms of the ratios shown in the following table:-

Table 1 ($M_{\pi N}$ <1.4 GeV)

	Experiment	$A_1 = 0$	Adler
$R^+ = \frac{\sigma(\mu^- n\pi^+)}{\sigma(\mu^- p\pi^\circ)}$	1.01 ± 0.33	0.5	0.77
$R^{++} = \frac{\sigma(\mu^- n\pi^+ + \mu^- p\pi^\circ)}{\sigma(\mu^- p\pi^+)}$	0.74 ± 0.15	0.33	0.58

Clearly, the absence of $I = \frac{1}{2}$ final states is completely excluded, and observed rates are in accord with the Adler computation.

IIb Multipion Production

A careful study[5] has been made of 2π and 3π production by the ANL-Purdue group. There is not space here to describe the identification of the many channels in detail, but Fig. 5 illustrates the type of results obtained for the exclusive cross-sections. The elastic, 1π, 2π and 3π channels are each characterized by a steep rise from threshold, with a levelling out at high energy on account of form-factor effects.

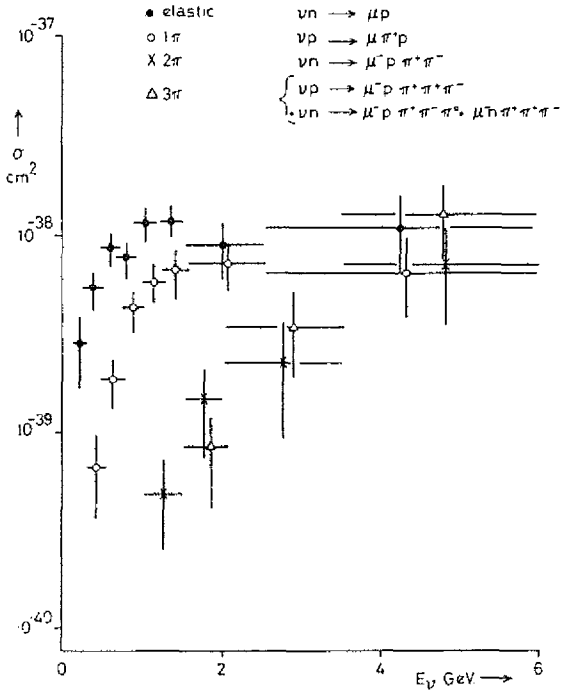

Fig. 5 cross-sections for some exclusive reaction channels measured by ANL-Purdue in deuterium and hydrogen.

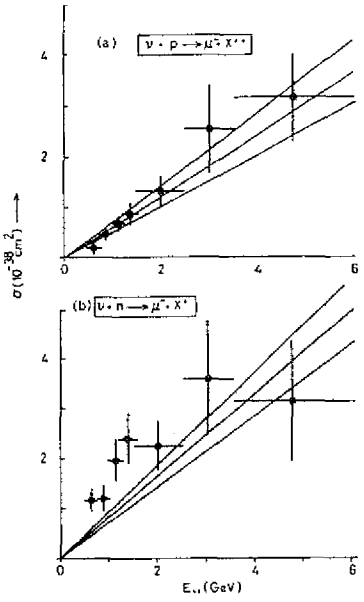

Fig. 6 Inclusive cross-sections observed by ANL-Purdue for reactions on (a) protons (b) neutrons. The straight lines indicate the slope of the fits to the CERN freon data, assuming a constant value $\sigma(\nu n)/\sigma(\nu p) = 1.40$.

III INCLUSIVE CROSS-SECTIONS

IIIa Cross-sections on Nucleons

The CERN Gargamelle total cross-section data were published in 1972[6], and recently a re-evaluation has been carried out with a threefold improvement in antineutrino statistics. These results are of interest, in the light of reported anomalies in differential cross-sections, as they illustrate some of the systematic errors which can arise in cross-section measurements with wideband beams. The measurements refer to neutron-proton averages in freon (CF_3Br, n/p = 1.19).

Fig. 7 shows the CERN ν, $\bar{\nu}$ spectra, and one notes the conspicuous "elbow" in the spectra at 5-8 GeV, where neutrinos from K-decay take over from those from π-decay. Because of the finite

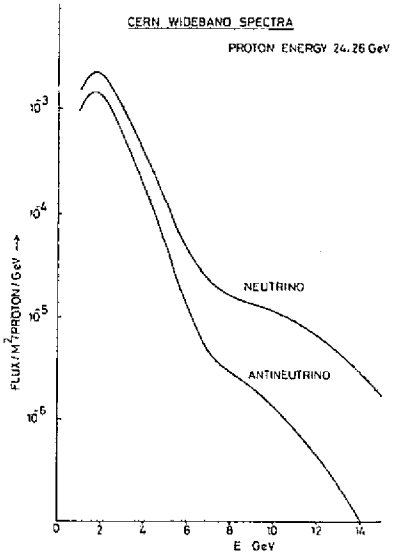

Fig. 7 The neutrino/ antineutrino fluxes in the CERN wideband experiments. The "elbow" in the curves around 6 GeV occurs where neutrinos from kaon decay dominate over those from pion decay.

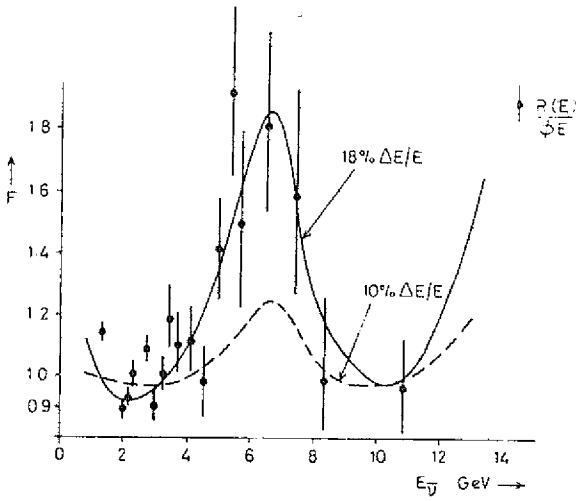

Fig. 8 The curves show the results of Monte-Carlo calculations of the expected ratio of observed event rate to the event rate which would be observed with perfect resolution. The experimental points are the (normalized) values of antineutrino event rate divided by the product of flux x energy.

energy resolution, this leads to "pile-up" effects for such a steeply-falling spectrum. This feature is illustrated in Fig. 8, giving the ratio F of the observed cross-section at energy E - that is, the number of events with measured anti-neutrino energy E divided by the flux factor - to the true cross-section which would

be obtained with perfect resolution. The curves show the variation F(E) expected, on the basis of a Monte Carlo calculation taking account of the energy resolution, $\Delta E/E$. Those for $\Delta E/E = 10\%$ and $\Delta E/E = 18\%$ are given as examples. The effect is second order in $\Delta E/E$ and thus varies rapidly with the resolution. In the actual experiment, the muon momentum resolution function is a Gaussian in $(1/p)$ with an rms deviation of 8%; while the hadron energy resolution is approximately Gaussian in E_{hadron} with rms deviation 16%. The curve marked 18% for brevity corresponds in fact to this case. Also shown is the observed event rate divided by the product of energy x flux. It is seen to follow approximately the variation expected from the Monte Carlo. The resolution should in principal depend on energy; however, examination of the internal momentum errors on individual secondaries indicates that, for the total secondary energy, there is no appreciable dependence of resolution on energy over the range 2-14 GeV, and we neglect such effects. The magnitude of the effects of resolution on total cross-sections provides a clear warning that distortions can arise in wideband experiments, and that apparent anomalies can have an instrumental rather than physical origin.

Fig. 9 indicates the results of the preliminary new analysis of the CERN data, including all necessary corrections for the effects of resolution as discussed above, subtractions for neutral current contamination and wrong sign muons etc. The analysis also involved other corrections; events were accepted only from completely measured rolls of film taken in "good beam" conditions, where flux data was reliable; badly-measured events (momentum error >30% on any secondary) were excluded and suitable loss corrections applied.

The errors shown in Fig. 9 are only statistical. There are, in addition, possible errors arising from flux uncertainties and rate corrections estimated to be ±7% for E = 2-8 GeV, and increasing to ±12% for E = 12 GeV; and those from the correction for the energy resolution, which are believed to be of the same order. Thus,

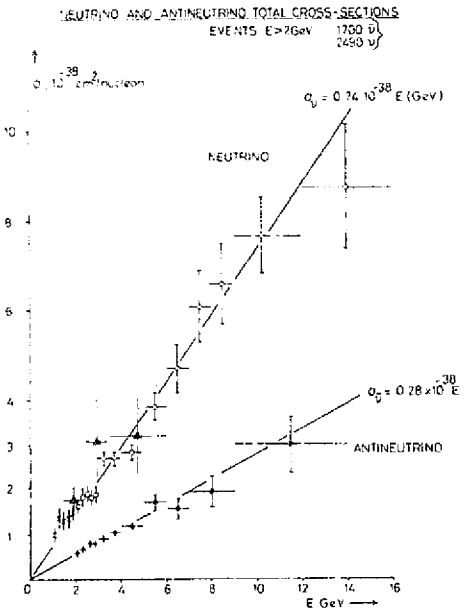

Fig. 9 Preliminary data on re-evaluation of the CERN GGM total cross-sections, corrected for energy resolution. The neutrino cross-section data below 2 GeV is taken from the earlier paper, and the lines are the previous linear fits. The triangles indicate neutron-proton average cross-sections from ANL.

in Fig. 9, the statistical errors should be increased by ∿50% in order to take account of systematic effects. The lines in this figure are the linear fits previously published[6]. Included in Fig. 9 are the nucleon-averaged total neutrino cross-sections from the ANL experiment, which are in good accord with the CERN values.

Fig. 10 shows the updated CERN values for the cross-section ratio $R = \sigma^{\bar{\nu}}/\sigma^{\nu}$. The ratio should be largely independent of some of the systematic effects, notable those from flux calibration and energy resolution corrections. The systematic uncertainty in R is estimated to be ±5%, as quoted previously. The mean value of R over the range 2-14 GeV is 0.37 ± 0.02, as compared with the value 0.38 ± 0.02 given previously.

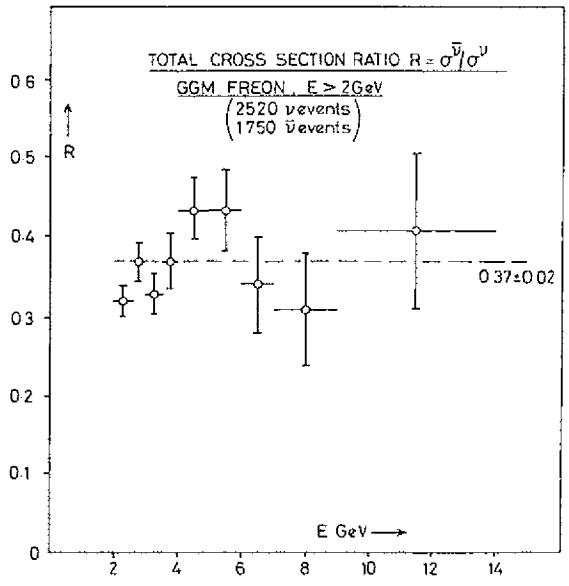

Fig. 10 The cross-section ratio obtained from the data of Fig. 9. The calibration errors are of order 5%.

At high energy, 20-200 GeV, total ν and $\bar{\nu}$ cross-sections have not as yet been determined with the precision of the low-energy CERN data. However, all the experiments to date (HPWF, CALTECH-FERMILAB, and the 15' hydrogen chamber data) are completely consistent with linearly-rising cross-sections to the highest energy. Furthermore, the values of the slope parameters in the CALTECH-FERMILAB narrow-band data are in agreement with the CERN numbers. (See the report of B. Barish at this conference.)

IIIb Neutron-Proton Cross-Section Ratios

Two measurements of $\sigma^{\nu n}/\sigma^{\nu p}$ in deuterium have been reported, from the ANL-Purdue collaboration[5] and from the BNL experiment (paper by N. Samios in these proceedings). Fig. 11 shows the ANL-Purdue ratio as a function of energy. Below 2 GeV, the elastic channel on neutrons tends to dominate and $\sigma^{\nu n}/\sigma^{\nu p}$ is correspondingly large. Table 2 summarizes all results to date. The CERN experiments

Table 2

Values of $\sigma(\nu n)/\sigma(\nu p)$

Laboratory	Energy	Ratio	Authors
(1) ANL (H_2,D_2)	E > 2	1.4 ± 0.3	Barish et al (1975)[5]
(2) BNL (H_2,D_2)	E > 1 ν > 0.8	1.4 ± 0.14 1.04 ± 0.16	Cazzoli et al (1975)[26]
(3) CERN GGM C_3H_8	E > 1	2.1 ± 0.3	Haguenauer (1975)[7]
(4) CERN 1.2 m. C_3H_8	E > 1	1.8 ± 0.3	Myatt and Perkins[8] (1971)
CERN 1.2 m CF_3Br	E > 1	1.3 ± 0.3	

(3) and (4) were in heavy liquid and attempted to identify the events on neutrons and protons – as is done in deuterium – on the basis of charge balance. Such methods involve unknown (and probably large) systematic errors on account of nuclear (charge-exchange) effects and the results are inherently much less reliable than the deuterium ratios. The cut in hadron energy ν > 0.8 GeV in the BNL data is intended to remove quasi-elastic events.

$\sigma^{\nu n}/\sigma^{\nu p}$ Predictions of $\sigma^{\nu n}/\sigma^{\nu p}$ are based on fits of quark/antiquark momentum distributions to electron scattering data. The values obtained range from ∿1.5 to ∿2.5, and apply of course to the deep inelastic region, whichis well above the typical energies of the present experiments.

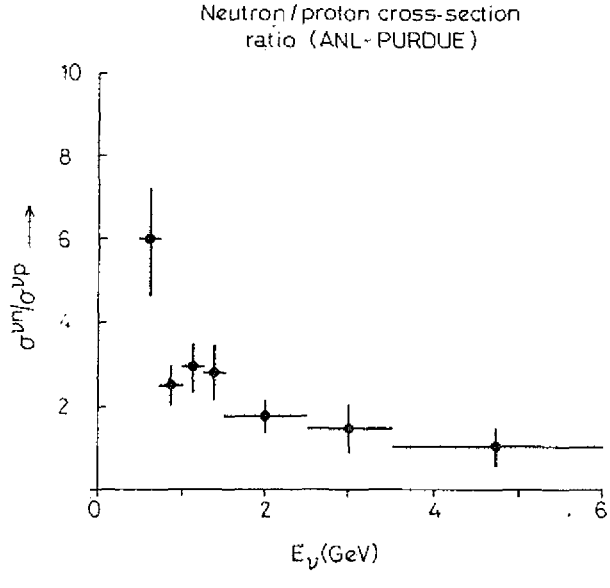

Fig. 11 Neutron/proton cross-section ratio for neutrinos, ANL-Purdue.

IV STRUCTURE FUNCTIONS AND SCALING

The CERN Gargamelle analysis of inelastic cross-sections in terms of the absolute values of the structure functions F_2 and F_3, has already been published[9] and we report here preliminary results from a re-analysis with improved statistics. The data is taken from runs in heavy freon (CF_3Br).

The analysis is carried out under the simplifying assumptions:-

(i) Charge symmetry invariance. This implies neglect of the Cabibbo angle ($\sin^2\theta_c = 0$) so that one can write $F_i^{\nu n} = F_i^{\bar{\nu}p}$, $F_i^{\bar{\nu}n} = F_i^{\nu p}$ $(i = 1,2,3)$.

(ii) $2x\,F_1(x) = F_2(x)$ (Callan-Gross relation).

(iii) Isoscalar target ($n/p = 1.19$ in freon).

The Bjorken cross-section is

$$\frac{d^2\sigma^{\nu,\bar{\nu}}}{dxdy} = \frac{G^2ME}{\pi}\left[\left(1 - y - \frac{Mxy}{2E}\right) F_2(x) + \frac{y^2}{2}\,2x\,F_1(x) \pm \left(y - \frac{y^2}{2}\right) xF_3(x)\right]$$

where $x = q^2/2M\nu$, $y = \nu/E$ and F_1, F_2 and F_3 refer to a neutron-proton average. The corrections for the finite Cabibbo angle, and the fact that the neutron-proton ratio is slightly different from unity have been discussed before[10]; they are at the level of $\sim$3% and can be neglected. The 1974 analysis was carried out with the "standard" SLAC scaling cuts $W^2 > 4$GeV , $q^2 > 1$ GeV; the results for F_2 and xF_3 are given in Fig. 12. Note that, because of the relatively low beam energy, there is little information for $x < 0.1$.

An attempt has been made to extend the values of F_2 and F_3 to small x, following the observations[11] at SLAC on the approach to scaling at low q^2. In electron-proton scattering, it has been found empirically that, at low q^2,

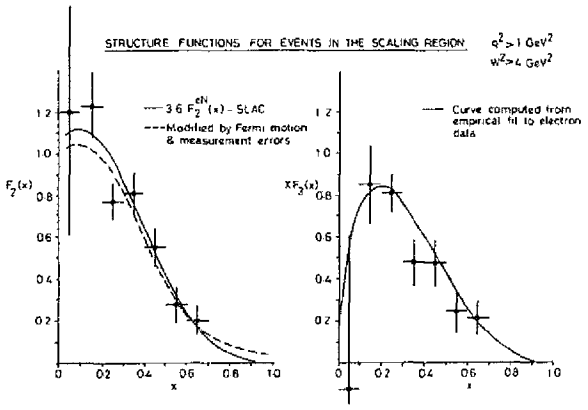

Fig. 12 Values of the structure functions $F_2(x)$ and $xF_3(x)$, evaluated in the scaling region $q^2>1$ GeV , $W^2>4$ GeV , as published by CERN GGM collaboration .

$$\underset{\uparrow}{\nu W_2^{ep}(x,q^2)} \quad \underset{\uparrow}{\approx} \quad \underset{\uparrow}{F_2^{ep}(x)} \cdot \left[1 - W_{e\ell}(q^2)\right] \qquad (4)$$

$W^2 > 4$, all q^2 — scaling region ($W^2 > 4$, $q^2 > 1$)

where F_2, the value of νW_2 in the scaling region, depends on x only, and $W_{e\ell}(q^2)$ is the structure factor for elastic scattering:-

$$W_{e\ell}(q^2) = [G_E^2(q^2) + (\mu^2 q^2/4M^2)G_M^2(q^2)]/[1 + q^2/4M^2] \qquad (5)$$

Here, μ is the proton magnetic moment (= 2.79 n.m.) and the elastic form factors have the usual dipole form

$$G_E(q^2) = G_M(q^2) = [1 + q^2/0.71]^{-2} \qquad (6)$$

The behaviour (4) is expected theoretically for proton targets in the closure approximation; it has not been tested experimentally for neutrons. It is not clear what is the appropriate correction in the neutrino case. If a similar ansatz applied to weak scattering on nucleon targets, we could write

$$\underset{\uparrow}{F_{2,3}(x)} = \underset{\uparrow}{F_{2,3}(x,q^2)} \left[1 - \frac{d\sigma_{e\ell}(q^2)/dq^2}{d\sigma_{e\ell}(0)/dq^2}\right]^{-1} \qquad (7)$$

scaling — $W^2 > 4$, any q^2

The elastic cross-section is however a function of neutrino energy E; in the high energy limit ($ME >> q^2$) it has the asymptotic form,

$$\frac{d\sigma_{e\ell}(q^2)}{d\sigma_{e\ell}(0)} = \{[1 + q^2\mu^2/4M^2]\, G_V^2 + \lambda^2 G_A^2\}/(1 + \lambda^2) \qquad (8)$$

where $\mu = \mu_p - \mu_n = 3.7$ n.m., $\lambda = 1.25$, and G_V and G_A are the axial and vector form factors. For simplicity however we have assumed that the corrections to the observer cross-sections are just given by

$$\underset{\uparrow}{\frac{d\sigma^{\nu,\bar{\nu}}(x)}{dx}} \underset{\uparrow}{\approx} \frac{d\sigma^{\nu,\bar{\nu}}}{dx}\,(q^2,x) \cdot \left[1 - \frac{1}{(1 + q^2/0.71)^4}\right]^{-1} \qquad (9)$$

scaling — $W^2 > 4$, any q^2

This formula involves somewhat smaller correction factors than (7) and (8); however, the difference is comparable with that arising from the uncertainty in G_A (see equation (1)) and arbitrariness in fixing the appropriate value of E. It turns out in fact that the statistical errors in the neutrino data are larger than these variations in the correction factors, in the low q^2 region where the effect is important.

The analysis has been carried out on 2212 neutrino events and 873 antineutrino events of energy 2.5 < E < 12 GeV, over which range the fluxes are known with fair precision. After applying the

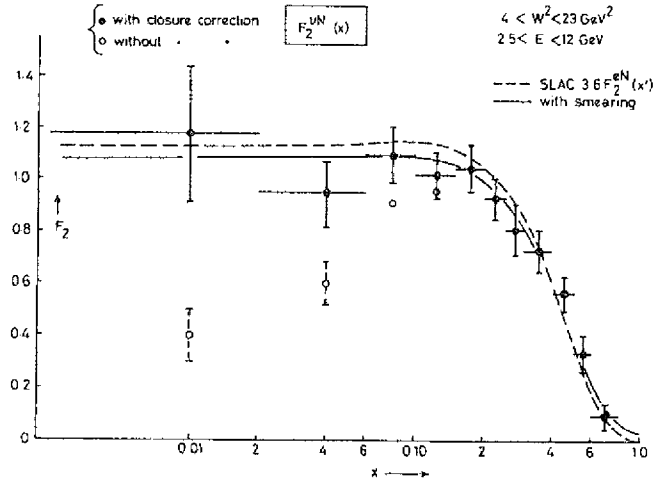

Fig. 13 Value of $F_2(x)$ evaluated for events of $W^2 > 4$ GeV and all q^2. Events with low q^2 have been weighted by the factor in equation (9). The curves are those from the SLAC experiments analysed in similar fashion. The results are preliminary.

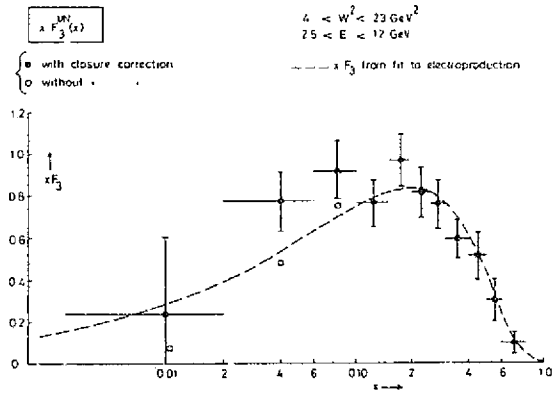

Fig. 14 $xF_3(x)$ evaluated from the CERN GGM events in the same manner as $F_2(x)$. The dashed curve was calculated from fits of quark distributions to electroproduction.[12]

cut $4 < W^2 < 23\ GeV^2$, 635 neutrino and 156 antineutrino events survived. $F_2(x)$ and $xF_3(x)$ were evaluated from the double differential cross-sections:-

$$F_2(x) = \frac{\pi}{G^2 M} \frac{\frac{1}{E}\frac{d^2\sigma^{\nu}}{dxdy} + \frac{1}{E}\frac{d^2\sigma^{\bar{\nu}}}{dxdy}}{2(1 - y + y^2/2)}$$

$$xF_3(x) = \frac{\pi}{G^2 M} \frac{\frac{1}{E}\frac{d^2\sigma^{\nu}}{dxdy} - \frac{1}{E}\frac{d^2\sigma^{\bar{\nu}}}{dxdy}}{2y(1 - y/2)}$$

after applying the correction (9). Particular attention was paid to the removal of background due to (i) neutral current events with a leaving π^+ or π^-, simulating a charged current event (ii) "wrong sign" charged current events - for example, a background neutrino event in antineutrino film, with a leaving π^+, simulating an antineutrino interaction. These backgrounds were evaluated from observations on unambiguous neutral and charged current events.

The resulting values of $F_2(x)$ and $xF_3(x)$ are shown in Figs. 13 and 14, computed with and without the weighting factor (9). In Fig. 13, the curve shows the electroproduction data[11] multiplied by the canonical quark-model factor 3.6, and "smeared" in accord with the measurement errors and for Fermi motion. The curve in Fig. 14 is deduced from an empirical fit of quark momentum distributions to the electroproduction data.[12,9]

Fig. 15 shows the y distributions obtained from the Gargamelle data. These were averaged over the range x = 0-0.4; the W^2 cut restricts the useful range of y from 0.2-1.0. It should be emphasized that the background corrections to antineutrino data are particularly severe at large y, since here, neutral current and wrong-sign muon background has its maximum effect. In the final bin y = 0.8 - 1.0, the antineutrino cross-section is reduced by almost a factor 2 from its raw value.

The curves in Fig. 15 are those deduced from the relative magnitudes of $\int xF_3^{\nu N}dx$ and $\int F_2^{\nu N}dx$ previously determined; the ratio is B = 0.80±.06, and this mean value for the V-A interference term provides a good fit, thus checking the internal consistency of the data.

The results of this preliminary analysis are summarized in Table 3:-

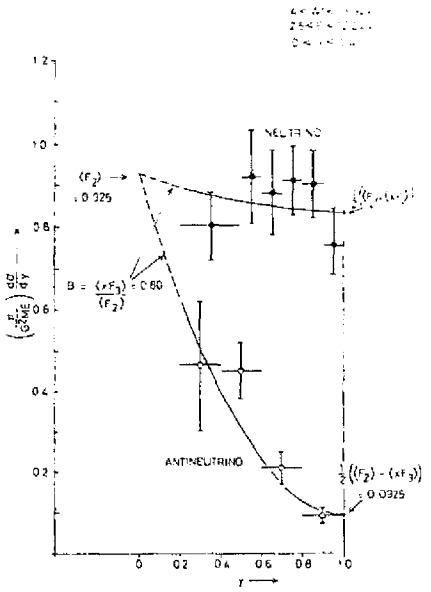

Fig. 15 The values of $(\pi/G^2ME)\, d\sigma/dy$ calculated from the CERN GGM data. The curves are those computed from the mean values of F_2 and xF_3 averaged over the range x = 0-0.4. Because of the cuts on W^2 and E, no useful data exists for y < 0.2. The data is corrected for neutral current and "wrong sign muon" background.

Table 3

Scaling Functions (CERN GGM)

$\int_0^{0.8} F_2^{\nu N} dx$	$\int xF_3^{\nu N} dx$	$\langle B \rangle = \int xF_3 / \int F_2$	$R = \langle \sigma^{\bar{\nu}}/\sigma^{\nu} \rangle$ scaling
0.47 ± 0.02	0.38 ± .03	0.80 ± .06	0.43 ± .04

Note that, contrary to what has sometimes been stated[15], the $\bar{\sigma}/\sigma$ ratio in the scaling region is not substantially different from the average value (Fig. 10) without scaling cuts, at least in this energy range.

In order to compare with the high energy data, we compute the moments of the neutrino/antineutrino x distributions in the scaling region:-

Table 4

	CERN GGM ($W^2>4$) νN	CALTECH/FNAL[13] νN	15' FNAL/MICH[14] νp	HPWF[15] νN
$\langle x \rangle^{\nu}$	0.26 ± 0.02	0.26 ± 0.02	0.22	0.22 ± .01
$\langle x \rangle^{\bar{\nu}}$	0.25 ± 0.02	0.19 ± 0.02	-	0.23 ± .01
$\bar{Q}/(Q+\bar{Q})$ $= (1-\langle B \rangle)/2$	0.10 ± .03	$0.10 \begin{smallmatrix} +0.13 \\ -0.09 \end{smallmatrix}$	-	-

On average, the mean values of x tend to be somewhat lower at the higher energies. This point is discussed later.

To summarize the CERN GGM data, we can conclude that:-

(i) The cross-sections observed are consistent with the hypothesis of charge symmetry.

(ii) The values of F_2 and xF_3 are in agreement with the quark model

(ii) predictions from electroproduction (or equivalent assumptions*), and this agreement seems to extend even into the region of low x ($\sim$.01).

(iii) The momentum fraction carried by (non-strange) antiquarks is 10%.

V STRANGE PARTICLE PRODUCTION

The general question of strange-particle production, and the lack of any evidence for anomalously high rates, which would signal new quantum numbers (charm), has already been discussed by B. Roe and N. Samios in these proceedings. Here I simply want to discuss the $\Delta S = 1$ rates in the context of the quark model and the antiparton densities in the nucleon.

Table 5 summarizes the information on strange-particle (SP) events yielding 3C kinematic fits in the hydrogen/deuterium experiments. In these cases only can one distinguish unambiguously between $\Delta S = 0$ associated production (AP) and $\Delta S = 1$ processes.

Table 5

Strange Particle Events giving 3C Fits

Laboratory	No. Events Total	No. SP Events	No. AP	No. $\Delta S=+\Delta Q$	No. $\Delta S=-\Delta Q$
ANL (νH_2, D_2)	$\sim$600	6	4	2(K^+,K°)	0
BNL (νH_2, D_2)	560	4	2	1(K°)	1 [16] ($\Lambda\pi^-3\pi^+$)
FNAL (νH_2)	500	5	5	0	0
	TOTAL	15	11	3	1

* The famous ratio $F_2^{\nu N}/F_2^{eN} = 3.6$ is predicted on more general grounds. From CVC, we expect $F_2^{\nu N}$(vector) = $2F_2^{eN}$ (isovector) = 1.8 F_2^{eN} (total), since in photoproduction, the isoscalar contribution is known experimentally to be $\sim$10%. Chiral symmetry($|V| = |A|$) would then predict $F_2^{\nu N}$ (V and A) = 3.6 F_2^{eN}. Note that $|V| = |A|$ is a necessary consequence of spin $\frac{1}{2}$ partons, and that the triplet quark model actually predicts 10% isoscalar contribution in electroproduction.

In two of the cases of single K production, a K°_{S} is observed. Thus they could be due to either K° or $\bar{K}^{\circ}$; I have assumed them to be K°. With this assumption, one can estimate very roughly the $(\Delta S = +\Delta Q)/(\Delta S = 0)$ cross-section ratio. Allowing for the K° detection efficiency (30%), and the fact that only half the total events will be above strange particle threshold (ANL and BNL) or be of low enough energy to yield 3C fits (FNAL), one finds

$$\frac{\sigma^{\nu}(\Delta S = +1)}{\sigma^{\nu}\ (\text{total})} \sim \frac{7}{1660/2} \sim 0.01$$

In the quark model, neutrinos must scatter off antiquarks in order to produce K^{+} and K°:-

$$\nu + \bar{p} \rightarrow \bar{\lambda} + \mu^{-}$$

$$\nu + \lambda \rightarrow p + \mu^{-}$$

The expected rate for such transitions will be (assuming an SU3-symmetric $Q\bar{Q}$ "sea"):-

$$(1 - B)\ \tan^{2}\theta_{c} = 0.01 \pm 0.003$$

for $\tan^{2}\theta_{c} = 0.05$ and the value of $\langle B \rangle = 0.80 \pm 0.06$ from Table 3. The data in Table 5 thus give further support to the quark model and the previous estimate of the "sea" contribution (Table 4).

VI ANOMALIES IN THE X AND Y DISTRIBUTIONS AT HIGH ENERGY

VIa The Distributions in x $(x = q^{2}/2ME_{\text{hadron}})$

The differences between some of the x distributions in the high energy neutrino/antineutrino at FNAL and those expected from the SLAC data have been emphasized previously[15]. These differences are illustrated by the first moments of the x distributions, summarized in Table 4. The values of $\langle x \rangle$ in the CERN GGM experiment are in good agreement with the expectations from the SLAC data, whereas the FNAL distributions are more peaked to low x. The 15' νp distribution and that from the HPWF experiment can be found in the reports by B. Roe and D. Cline respectively. The neutrino data from two FNAL experiments and the CERN experiment, all normalized to the same area, are shown in Fig. 16, together with the predicted shape from the Bodek fit to the SLAC data.

One should remark that the FNAL bubble chamber data is on hydrogen, whereas the rest refer to isoscalar targets. A slightly

more peaked distribution is therefore expected in the former case. Furthermore, it is precisely in the region of small x that the major background corrections for neutral current events are required in the hydrogen bubble chamber data, since at low q^2 the identification of the outgoing muon is least certain. Typically, the correction in this region is 20% or more. Hence the main discrepancy rests with the HPWF data, which indicates a significant excess of events for x = 0.1 - 0.2. A similar situation obtains in that experiment with the antineutrino x distribution.

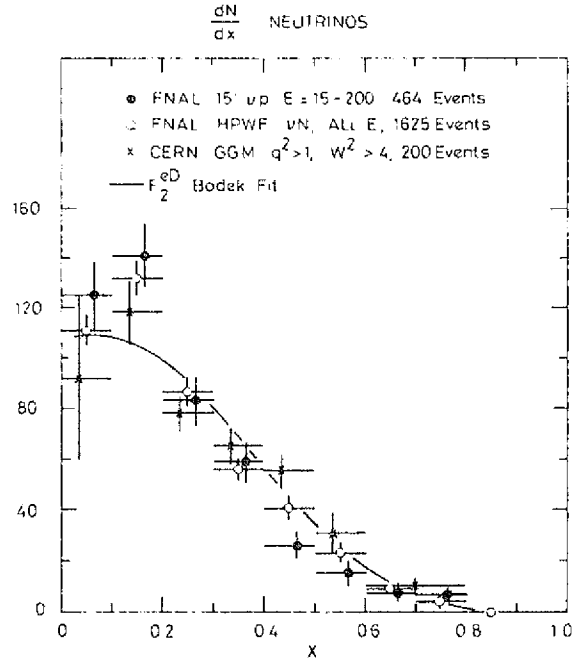

Fig. 16 The x distributions for neutrinos. The curve is a fit to the electron-deuteron data at SLAC. Note that the two high energy experiments at FNAL indicate an excess of of events for x <0.2 and a deficit for x > 0.2. All distributions are normalized to the same area.

While it would be unwise to conclude too much about the high energy data until there is better consistency between the various experiments, which have widely different problems regarding geometrical acceptance, background, and resolution, there are certainly indications of departures from the scaling distributions of the low energy electroproduction data. The reported departures from scaling in high energy muon scattering[17] are in the same direction as these effects, and lead also to x-distributions peaked to lower x at higher q^2 values.

Obviously, changes in <x> with energy will be reflected in changes in the slope of the ν-plot ($\langle q^2\rangle/E = 2M\langle\nu\rangle = 2M\langle xy\rangle$), which are also observed.

IVb Anomalies in y Distributions ($y = E_{hadron}/E_o$)

The most striking anomalies in the high energy data have been reported in the antineutrino y-distributions by the HPWF group in their Fermilab experiments.[15,18,19,20] Fig. 17 shows the most recent data[15]. The y-distributions for neutrinos are flat, for all x values and all energies. The antineutrino distribution,

for $x > 0.1$, falls off as $(1-y)^2$, whereas for $x < 0.1$, the distribution is consistent with being flat. According to our present ideas, distributions which are flat, or go as $(1-y)^2$, represent the two absolute extreme cases; it is hard to imagine any physical process which, averaged over a large neutrino energy range, will cleanly separate the y dependence into these two extreme distributions, simply by a cut in x. Therefore, the curves shown in Fig. 17 should not be taken too literally as representing the data; the observed points are also consistent with a more rapid fall off with y for $x < 0.1$, and a less rapid fall-off for $x > 0.1$. It should also be pointed out that the Caltech-Fermilab experiment[13], with however much poorer statistics, does not observe evidence for such anomalous behaviour - see Fig. 18.

In the HPWF data, the relative normalization of the neutrino and antineutrino samples has been adjusted so that, for $x > 0.1$, dN/dy at y = 0 is equal for neutrinos and antineutrinos (in accord with charge symmetry).

There are two distinct aspects of the HPWF anomaly in the region $x < 0.1$:-

(i) The y distribution for antineutrinos appears to be flat.

(ii) At $y \sim 0$, dN/dy for antineutrinos is smaller, by a factor ~ 3, than that for neutrinos. Obviously, this effect depends on the normalization procedure, whereas (i) does not.

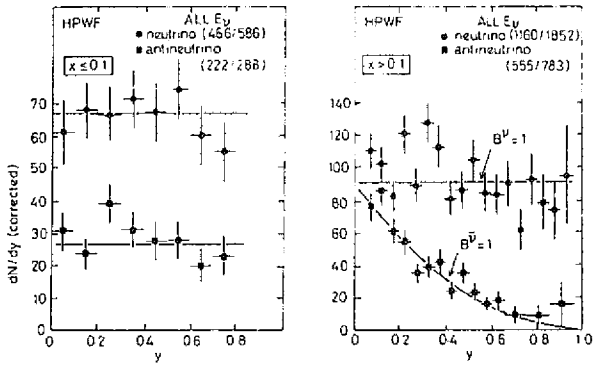

Fig. 17 Corrected y distributions for neutrinos and antineutrinos in the HPWF experiment[15], showing the anomalous behaviour of the antineutrino distribution for $x < 0.1$. The figures in brackets give the observed and the corrected numbers of events in each sample. The relative numbers of neutrino and antineutrino events are normalized by requiring that, for $x > 0.1$, the two cross-sections should be equal at $y \sim 0$.

Regarding the feature (i), it has sometimes been suggested that the flatness of the y distribution can be attributed to large antiparton contributions at small x (for equal parton/antiparton contributions, the y distribution would have the form $(1-y+y^2/2)$ for both neutrinos and antineutrinos). There is no evidence however that antipartons could have such a big effect. As an example, Fig. 19 shows the ratio $(d\bar{\sigma}/dx)/(d\sigma/dx)$ in the scaling region deduced from the CERN GGM data on F_2 and xF_3 (Figs. 13 and 14). The ratio is about 0.4 everywhere except possibly at very small x (<0.02), and

clearly the assertion that $Q \sim \bar{Q}$ for $x < 0.1$ is completely inconsistent with this data. It is of course possible that the "sea" contribution is larger at the higher energy, but it is impossible to verify this directly without reliable and detailed measurements of the cross-section ratio as a function of x.

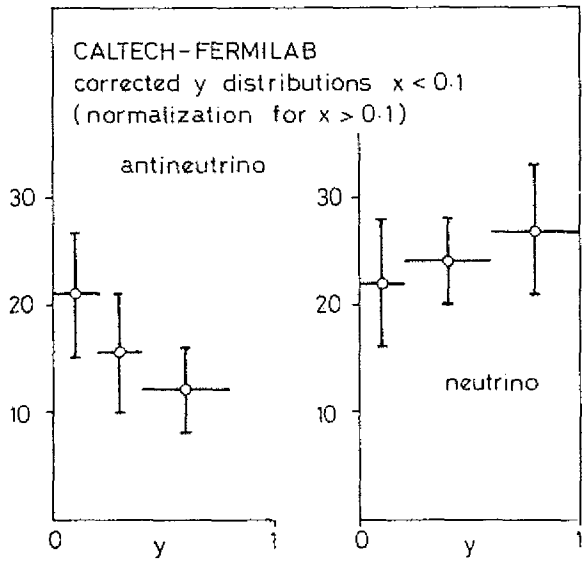

Fig. 18 y distributions for $x < 0.1$ observed in the Caltech-Fermilab experiment. Normalization procedure as in Fig. 17

The difference in magnitude (ii) of the neutrino and antineutrino cross-sections at small y is the more crucial aspect of the data, since it implies a severe violation of charge symmetry. The reason for this is that, independent of scaling, q^2 or ν cuts, or the Callan-Gross relation, any admixture of V and A coupling, together with the hypothesis of charge symmetry, leads to the following positivity constraints:-

$$(1 - y)^{-2} \geq \frac{\bar{\sigma}(q^2,\nu,y)}{\sigma(q^2,\nu,y)} \geq (1 - y)^2$$

Thus, for $y = 0$, $\sigma = \bar{\sigma}$ is a necessary consequence of charge symmetry, and the observation $\bar{\sigma} \sim \sigma/3$ is a clear and unambiguous indication of a large violation. (It should be noted that, to the extent that the Cabibbo angle is non-zero, the cross-sections in the conventional model also violate charge symmetry, but only to the extent of $\sin^2\theta_c \sim 5\%$).

It is appropriate to point out that the apparent breakdown of charge symmetry in the HPWF experiment occurs in the region of low q^2 and ν; for example, the first point in the antineutrino distribution for $x < 0.1$ has average values $x = y \sim 0.05$; thus, taking the mean energy as ~50 GeV, these events will typically have values of $q^2 \sim 0.25$ and $\nu \sim 2.5$. This region is also covered by the CERN data (but at a lower energy and correspondingly higher y values), where no violation of charge symmetry is apparent. If the effect is associated with the nucleon vertex, it should depend only on q^2 and ν, and thus the discrepancy is surprising. However, energy-dependent effects could arise at the lepton vertex (e.g. new lepton production).

The HPWF anomaly of course appears in other forms if the data is analysed in different ways, for example in plots of W or of $d\sigma/dq^2$. The difference of the last quantity for neutrinos and antineutrinos is related to the Adler sumrule[21]. For a purely isoscalar target, this states that, at fixed q^2,

$$\underset{E \to \infty}{Lt} \frac{\pi}{G^2}\left[\frac{d\sigma^{\nu N}}{dq^2} - \frac{d\sigma^{\bar{\nu}N}}{dq^2}\right] = A \qquad (10)$$

where the quantity A is a direct measure of the deviation from charge symmetry invariance[25]. Thus $A = 0$ in the GIM (SU4) quark model, and $A = -(3\sin^2\theta_c)/2 = -0.07$ in the GMZ (SU3) model. Although the nuclear targets (Fe, liquid scintillator, freon CF_3Br) considered here have $n/p \neq 1$, the net deviation of A from zero is less than 0.1 in these models. In some hadron models, A can be large; for example A=1.5 in one model with an extra (V + A) piece to the charm current[22].

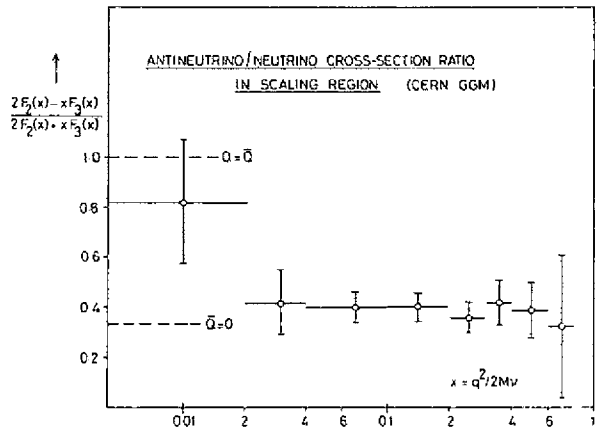

Fig. 19 The value of $\bar{\sigma}/\sigma$ plotted as a function of x, and applying to the scaling region. The ratio is calculated from the values of F_2 and xF_3 (Figs. 13, 14). In the quark model, a ratio of $1/3$ is expected in a region of x containing quarks only, and a value of 1 where there are equal quark and antiquark populations. Antiquarks appear to be important only at very small x.

In the scaling limit, the Adler sumrule may be written in the alternative form, setting $V = q^2/2ME$:-

$$\underset{V \to 0}{Lt} \frac{\pi}{G^2}\left[\frac{d\sigma^{\nu N}}{dq^2} - \frac{d\sigma^{\bar{\nu}N}}{dq^2}\right] = A \qquad (11)$$

scaling

This form is more convenient in practice than (10) since, on account of "precocious scaling":-

$$\frac{d\sigma}{dq^2} = \frac{d}{d\nu}\,(\sigma/2ME) = \frac{1}{N}\frac{dN}{d\nu}\cdot\frac{\alpha}{2M} \qquad (12)$$

where N is the total number of events in the sample, α the slope of the linear energy dependence of the total cross-section. In fact, when $d\sigma/dq^2$ is plotted as a function of ν, the distribution appears to be almost energy-independent - see Fig. 20. Thus, this form is useful for comparing the low and high energy data, even though neither will be in the scaling region in the limit of very small ν.

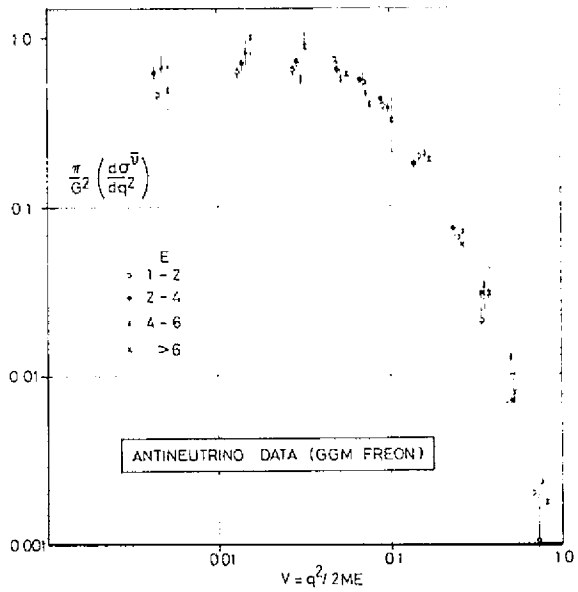

Fig. 20 The variation of $d\sigma/dq^2$ with $\nu = q^2/2ME = xy$ for anti-neutrinos. For all energies in the range 1-12 GeV, the points tend to fall on a universal curve, as expected from precocious scaling.

Fig. 21 shows the quantity $(\pi/G^2)(d\sigma^{\nu}/dq^2 - d\sigma^{\bar{\nu}}/dq^2)$ plotted as a function of ν for different energies, using the CERN[9] and HPWF[15] data*. While the two sets of data are in excellent agreement for $\nu > 0.1$, the CERN data converge towards zero as $\nu \to 0$, while the HPWF data actually reach a maximum there. Note that the variation with energy inside each data set seems to be small, and it appears therefore there is more likely a real discrepancy between the experiments, rather than a gradual transition from the low energy to the high energy region.[29]

The large intercept at $\nu = xy = 0$ in the FNAL experiment is of course a necessary consequence of the abnormally low anti-neutrino cross-section at small y and small x. (The entire effect in Fig. 21 is accounted for by a deficit of about 50 events ($y < 0.2$, $x < 0.1$) out of a total of about 1000 (see Fig. 17).)

---

* As far as is known, the same coefficients α were assumed in the two analyses: $(\pi/2MG^2)\,\alpha = 0.24$ for neutrinos and 0.090 for antineutrinos (Fig. 9). The CERN GGM data in Fig. 21 includes new results of greater statistical weight than those given by Deden et al.[9]

It is of importance here to emphasize that the total cross-sections and cross-section ratios required in the Fermilab analysis have been assumed and not measured directly; that quite drastic changes to the assumed values of α or R would be needed to remove the anomaly at $\nu = 0$; and that the agreement with the CERN results for $\nu > 0.1$ would then be destroyed. Leaving aside the Adler sumrule, it is also fair to point out that the anomaly in the y distribution itself disappears if the cut at $x = 0.1$ is removed. Fig. 22 shows the total HPWF antineutrino data, together with that, at similar energy but of much inferior statistics, observed by the ANL-Carnegie-Mellon group[14] in the 15' chamber ($\bar{\nu}p$). The curve is for $\langle B \rangle = 0.8$ as observed in the CERN GGM experiment. All three experiments are now compatible with a unique value of $\langle B \rangle$.

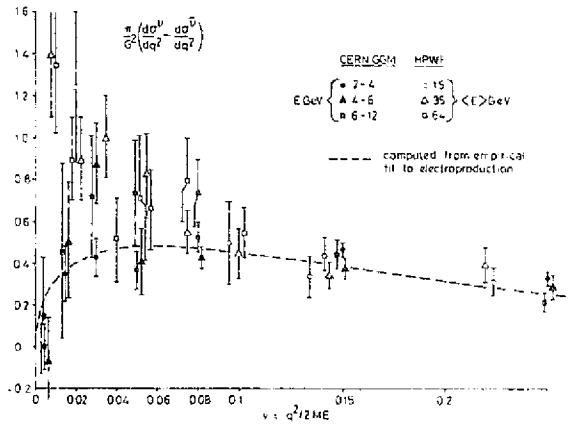

Fig. 21 The differential cross-section difference $(\pi/G^2)(d\sigma/dq^2 - d\bar{\sigma}/dq^2)$ as a function of $\nu = q^2/2ME$. Data is given in various energy bins, from the CERN GGM and HPWF experiments. As $E \to \infty$, the intercept at $\nu = 0$ is given by the Adler sum rule. The large value of the intercept in the HPWF data is associated with the abnormally low anti-neutrino rate for $x < 0.1$ and $y < 0.2$ in Fig. 17.

When the same procedure is applied to the neutrino data (Fig. 23) the distributions obtained are not very flat (as usually supposed) or even monotonic, and indeed give poor χ^2 fits for any value of $\langle B \rangle$. These results are given simply to illustrate the experimental problems in determining reliable y distributions. The data give a vivid impression of the experimental uncertainties; for example, in the bubble chamber data, there is severe background arising from neutral currents, distortions due to energy measurement errors etc., and the correction factors which have to be applied to the raw data are stated to be as large as 40% at large y. As mentioned previously, corrections to the raw cross-sections at large y in the GGM antineutrino data (Fig. 15) are even bigger than this.

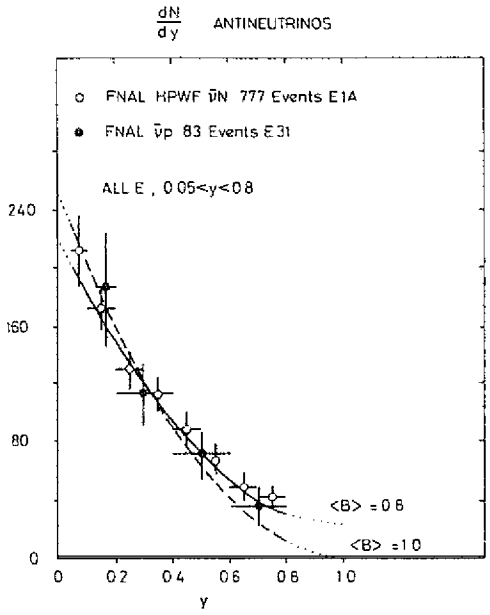

Fig. 22 Corrected y distributions from FNAL antineutrino data without x cuts. The curve <B> = 0.8 is a good fit to the CERN data (Fig. 15).

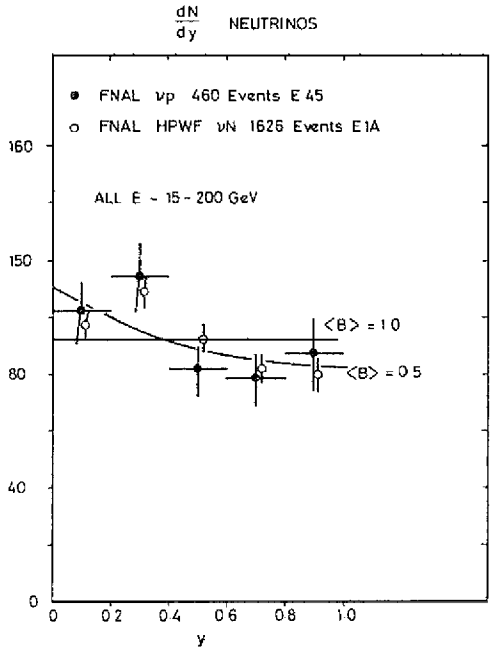

Fig. 23 Corrected y distributions for FNAL neutrino data. No single value of <B> gives a good fit to the data, presumably reflecting the existence of uncertainties in the corrections applied. The corrections in the νp bubble chamber data are substantial (∿40% at large y).

VIc Conclusions on the x and y Distributions

It is difficult to draw any very reliable conclusions in the present highly confused state of the inelastic data. However, one can make the following remarks:-

(i) Several experiments see indications of an enhancement of the cross-sections at small x (<0.2), or of a depletion at large x, relative to the SLAC scaling distributions. The general trend is in the same direction as that reported in inelastic muon scattering.

(ii) Large anomalies in the antineutrino y distributions at high energy and small x have been observed (HPWF), but these results are not so far confirmed by the CALTECH or FNAL bubble chamber experiments, and appear to lead to some inconsistencies with the CERN data, where it is possible to make a valid comparison.

(iii) The existence of the dimuon events shows that new physical processes must occur at high energies, and these will almost certainly lead one to expect some deviations in x and y distributions, sumrules etc. However, it is not certain that these deviations will be sufficiently large to be clearly distinguishable from the instrumental errors common to all the neutrino experiments.

(iv) Particularly in the high energy experiments, there is an obvious and serious mismatch between the statistical weight of the event numbers - several 1000 in the HPWF case - and the precision with which absolute or relative cross-sections ($\sigma^{\bar{\nu}}/\sigma^{\nu}$) are known. Thus, determination of cross-section differences may be subject to very considerable errors, both in absolute magnitude as well as in energy dependence. It also goes without saying that the measurement of absolute values of differential cross-sections, using measured fluxes, rather than shapes of distributions, will eventually have to be undertaken in order to quantify any new phenomena, and enable a proper confrontation with theoretical models.

VII LONG-LIVED HEAVY NEUTRAL LEPTONS

VIIa The Kolar Gold Field Experiments

In a recent paper, Krishnaswamy *et al*[23] have reported evidence for new processes, appearing as multitrack events close to the detectors in deep underground cosmic neutrino experiments at the Kolar Gold Fields (KGF) in S. India. The apparatus employed[24] consisted of arrays of scintillators, iron plates and neon flash tubes arranged in 5 telescopes of area 25 m^2, operated over several years. Fig. 24 shows an example of one of the 5 curious events.

In the experiments at KGF and similar ones in S. Africa (Case-Witwatersrand-Irvine), single tracks (muons) at zenith angle greater than 50° are attributed to interactions of atmospheric neutrinos in the surrounding rock, and the observed event rates are consistent with those expected. However, in the KGF experiment, out of a total of 20 events, 8 have more than one track (either 2 or 3). This multitrack rate is rather high. The expected proportion of muons with accompanying hadrons is <10%, since the mean range of a neutrino-produced muon is of order 5-10 m of rock, that is large compared with the hadron absorption length. Even more surprising is the fact that 5 of the 8 multitrack events have vertices close (<1m) to the detectors and possibly in the air of the tunnel. They have been attributed to the decay of new particles of mass ~2 GeV, giving several tracks at wide angles.

The authors[23] suggest that the particles responsible for these events have lifetimes of order 10^{-9} sec and are produced locally in neutrino collisions in the rock. The hypothesis has to meet the difficulty that the cross-section for producing the

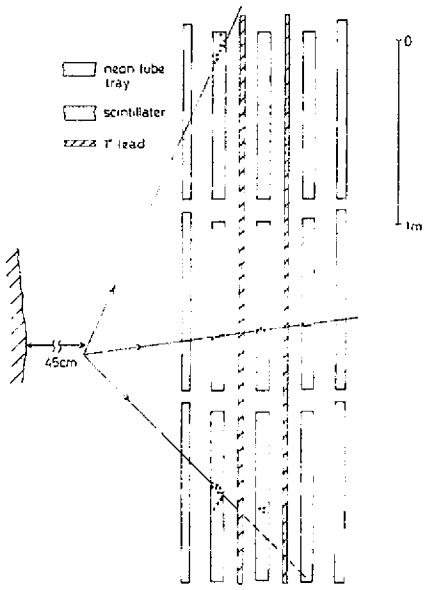

Fig. 24 An example of one of the multitrack events in the Kolar Gold Field (KGF) neutrino experiment, observed at 7600' depth (700 Kg/cm^2). Trajectories are indicated (in projection) by neon flash tubes.

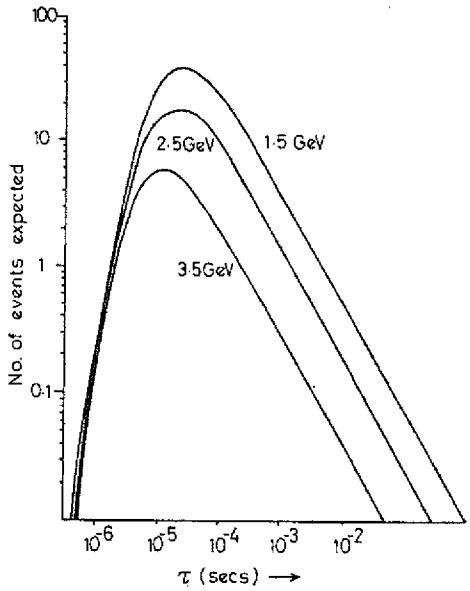

Fig. 25 The expected number of KGF events computed by de Rujula, Georgi and Glashow, assuming they are due to decay of long-lived neutral leptons created in the atmosphere. The curves are for different lepton masses. The observed number of events provide limits on the mass and the lifetime, τ.

new particles has then to be comparable with the total neutrino cross-section; further, since the bulk of the neutrinos have energies below 10 GeV, such effects should have been detected at accelerators.

Another explanation has been put forward by de Rujula, Georgi and Glashow[26]. They propose that the events are not of local origin, but due to decay of penetrating, long-lived neutral leptons L°, which themselves originate from decay in the atmosphere of charged leptons $L^\pm$. These charged leptons are produced electromagnetically in pairs in stratospheric collisions of primary cosmic ray protons. Fig. 25 shows the results of the computation of de Rujula et al, indicating that the observed event rate might be accounted for by a

lepton mass 2-3 GeV and L° lifetime $\sim 10\mu$sec. As these authors themselves stress, the calculated rates are very dependent on the model employed to describe lepton pair production.

VIIb Accelerator Experiments

The cosmic ray results can be compared rather directly with those from accelerator experiments in the light of the above (or some other) theoretical model. In Table 6 below I have summarized the results from the various laboratories and detectors, as far as they are known. The first row gives the proton energy and the number of incident protons on target. In the cosmic ray run, the local vertical geomagnetic cut-off energy is 16 GeV for protons. The effective number of protons is $\pi I_o St$ where I_o = omnidirectional intensity (I_o = 100 protons $m^{-2}sec^{-1}sterad^{-1}$ above cut-off), $St = 7.10^9 m^2 sec$ is the product of detector area and running time. The second row in the table gives the type of beam and target. The CERN run[27] consisted of a beam dump experiment, the protons being transported through a vacuum pipe on to a mercury target at the front of the shield, thus reducing the usual neutrino flux by a factor 10^3.

In all the other experiments, a normal neutrino target-decay path-shield layout was employed. In the HPWF experiment[28] a section of the calorimeter was emptied of liquid scintillator, so that any events recorded would occur in helium gas or in aluminium separator plates. The third row in the table specifies the solid angle $\Delta\Omega$ subtended by the fiducial cross-sectional area of the detector at the proton target.

The geometrical acceptance (proportion of heavy leptons produced which traverse the detector) depends on the model assumed for lepton production, as well as the lepton mass. Assuming, conservatively, that the leptons $L^\pm$ are produced isotropically in the CMS, and decay isotropically to L°, the acceptance goes roughly as the product $E_p\Delta\Omega$ and lies in the range 10^{-3}-10^{-4} for all the accelerator runs. For the KGF experiment, which employs an extended rather than a point proton source, the acceptance is unity. The product of proton intensity and acceptance is $2.10\ 10^{12}$ for the KGF run and 10^{13}-10^{14} for those at the machines. The length of the fiducial volume available for recording decays is about the same, of order 2m, in all the experiments. Thus, the sensitivity of each of the four accelerator runs is 10-100 times that of the KGF run, independent of the lepton lifetime τ, provided $\tau > 1\mu$sec. The fifth row of the table indicates the maximum lepton mass to which each experiment is sensitive. Only in the FNAL experiments would leptons of mass >3 GeV be produced.

Table 6

Cosmic and Accelerator Data on Neutral Lepton Search

	CERN (GGM)	ANL 12'	FNAL 15'	FNAL 1A	KGF (13°N)
E_p (GeV)	26	12.5	300	300	>16
N_p on target	4.10^{16}	6.10^{17}	4.10^{17}	2.10^{17}	2.10^{12}
BEAM	DUMP ($\nu,\bar{\nu}N$)	νH	νH	$\nu,\bar{\nu}N$	$\nu,\bar{\nu}N$
Target → Detector (m)	24	12	1400	1400	8500 sec θ
$\Delta\Omega_{lab}$	2.10^{-3}	5.10^{-2}	6.10^{-6}	2.10^{-6}	1.0
Integrated ν Intensity	10^{11}>1 GeV (10^{-3} normal)	10^{14} (>1 GeV)	10^{14} (>10 GeV)	10^{14} (>10 GeV)	10^{12}>2 GeV 10^{11}>10 GeV
$M^{max}_{L^{\pm}}$	3 GeV	1.9 GeV	>3	>3	-
N_{event}	2(1.5)	-	-	2(2.4)	5
Q = 0	0	0	0	-	

KGF experiment: N_p x geom. acceptance = 2.10^{12}

Accelerator experiments: N_p x geom. acceptance = 10^{13}-10^{14}

The result of the CERN GGM beam dump experiment[27] was that, out of some 40 events involving a secondary pion or muon, only 2 occurred in the downstream half of the fiducial volume, and had net longitudinal secondary momentum $p_x > 0.3$ GeV/c. They had configurations $p\pi^\circ\mu^+$ and $pp\mu^+$ respectively, with energies 2.4 GeV and 1.2 GeV. Neither can be due to decay of a neutral particle ($\Sigma Q = 0$); the expected number of interactions due to the residual $\nu/\bar{\nu}$ flux was 1.5.

In the HPWF experiment,[28] 2 events were recorded in the fiducial volume, both with an even prong number - thus possibly of $\Sigma Q = 0$ - and energies 4 and 7 GeV. 2.4 events were expected from ν, $\bar{\nu}$ interactions in the aluminium foils. In the ANL and FNAL hydrogen bubble chamber experiments, no events with even prong number have been recorded.

In summary therefore, the accelerator experiments observe no events, or no events above the expected background, which can be attributed to decay of neutral long-lived leptons. Furthermore, in case such neutral particles were locally produced by neutrinos, it should be pointed out that the integrated neutrino intensities through the detectors in these runs are 2-3 orders of magnitude in excess of those in the cosmic ray experiment. These completely negative results, involving sensitivities much greater than in the KGF experiment, are clearly in conflict with the observation of 5 cosmic ray events. It is therefore necessary to look more critically at the cosmic ray data. It is unfortunately clear that interpretations other than those of Krishnaswamy et al need to be considered. As an example, Fig. 26 shows one of the events, recorded in this case in an iron core spectrometer at a shallow level (3650'). Rather than the decay of an upward travelling particle decaying to 3 secondaries, it is possible that this event could be attributed to a downward travelling, wide zenith angle (50°) atmospheric muon which interacts electromagnetically in the last scintillator, and from which branch off several electron secondaries.

From the various accelerator experiments, some limits can be set on the properties of any new heavy leptons:-

(i) If the process envisaged is decay of a neutral lepton L°:-

$$p + \text{nucleus} \rightarrow L^\pm + \text{---} \ , \ L^\pm \rightarrow L^\circ \rightarrow \text{decay}$$

then the expected number of decays is of order

$$N_{expected} \sim \frac{10^{38}\,\sigma(\text{production})}{\tau(\mu\ \text{sec})}$$

where σ is the production cross-section of $L^{\pm}$ in collisions of protons in the target (or of the pions in the ensuing cascade), and where it is assumed that the L° lifetime $\gtrsim 1\mu$sec, so that a substantial fraction of L° will survive to the detector. Thus assuming the reasonable estimate of $\sigma = 10^{-34}\text{cm}^2$ for electromagnetic production of lepton pairs, lifetimes in the range $10^{-6} \to 10^{-1}$ sec are excluded. This result applies for lepton masses at least up to 5 GeV.

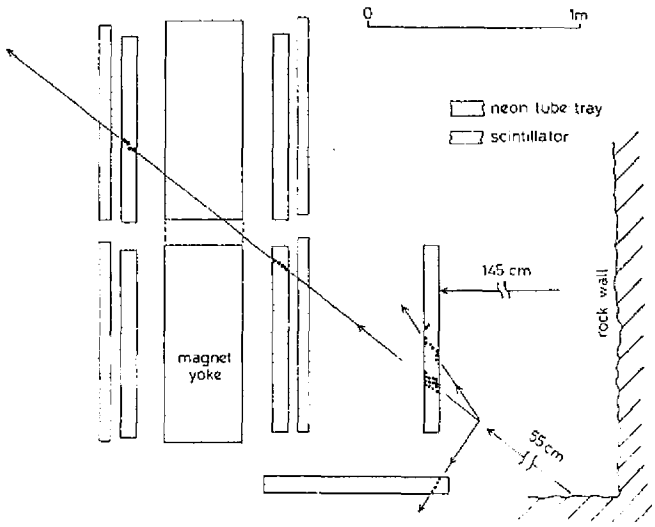

Fig. 26 Example of a multitrack event in the KGF experiment, observed in the magnet spectrometer array at 3650' depth (340 Kg/cm^2). At this smaller depth, atmospheric muons, even at 50° zenith angle, may be important. It is conceivable that the event could be due to a downward-travelling atmospheric muon undergoing electromagnetic interaction in the RH scintillator, giving electrons and γ-rays producing the tracks in the neon tubes at right.

(ii) If the process involved is the interaction of a long-lived penetrating neutral lepton produced near the target (e.g. a new neutrino ν_L associated with L), then the CERN beam dump experiment sets the limit

$$\sigma_{prod} \cdot \sigma_{int.} \lesssim 2.10^{-69}/\eta\ \text{cm}^4$$

where η is the geometric acceptance of the detector, which is in the region of 0.01. Thus, for an interaction cross-section $\sigma_{int} \sim 10^{-38}\text{cm}^2$, $\sigma_{prod} < 10^{-29}\text{cm}^2$. This result applies to lepton masses <3 GeV.

Finally, it is of interest to remark that neutrino experiments, particularly those of the beam dump variety, offer the possibility of exploiting the maximum accelerator luminosity in a search for new and rare processes with detectors of very large mass. Their drawback of course is that any such new particles produced at or near the proton target must be able to penetrate the muon shield, and such experiments are therefore not sensitive to particles of $\tau < 1\mu$sec or with interaction cross-sections $>10^{-28}\text{cm}^2$.

In summary, the Table 7 below shows existing limits on heavy leptons from neutrino experiments.

Table 7

Heavy Lepton Limits; Neutrino Experiments

Type of Heavy Lepton	Reaction	Experimental Limit
Heavy Muon M^+	$\nu_\mu + N \to M^+ + \ldots$ $\hookrightarrow e^+ \nu_e \nu_\mu$ (15%) $\hookrightarrow \mu^+ \nu_\mu \nu_\mu$ (30%)	 $M > 2.1$ GeV* $M > 7$ GeV†
Heavy Electron E^+	$\nu_e + N \to E^+ \ldots$ $\hookrightarrow e^+ \nu_e \nu_e$	No Useful Limits
Sequential Lepton	$\nu_\mu + N \to L^\pm + \nu_L + \nu_\mu$	Unobservable?
	$p + N \to L^+ + L^- + \ldots$, $L^+ \to \nu_L + \ldots$; ν_L interacts $L^+ \to L^\circ + - -$; L° decays	 $\sigma_{prod.} \sigma_{int} < 10^{-67} cm^4$ $10^{-1} sec < \tau_{L^\circ} < 10^{-6} sec$

* Deden et al, Phys. Lett. 46B, (1973) 281 revised value.

† B. Barish et al, Proc. XVII Conf., IV-147 (London 1974.

ACKNOWLEDGMENTS

I am indebted to the Gargamelle collaboration and to the FNAL, Michigan, ANL, Purdue and Carnegie-Mellon bubble chamber groups, for permission to quote unpublished data; to R. Stefanski for details of the HPWF heavy lepton search experiment; and M. Derrick and F. Nezrick for similar details from the ANL and FNAL bubble chamber experiments.

REFERENCES

1 S.J. Barish et al (ANl-Purdue). Submitted paper
Also W.A. Mann et al, Phys. Rev. Lett. 31, 844 (1973)

2. Rollier (GGM collaboration) La Physique due Neutrino a Haute Energie, p.349 (CNRS, Paris 1975).

3 S.J. Barish et al ANL-HEP-PR-75-36

4 S.L. Adler, Annals of Physics 50, 189 (1968); also
P. Schreiner and F. von Hippel, Nucl. Phys. B58, 333 (1973).

5 S.J. Barish et al ANL-HEP-CP-75-38.

6 T. Eichten et al Phys. Lett. 46B, 274 (1973).

7 M. Haguerauer (GGM collaboration), La Physique due Neutrino a Haute Energie, p.327 (CNRS, Paris 1975).

8 G. Myatt and D.H. Perkins, Phys. Lett. 34B, 542 (1971)

9 H. Deden et al Nucl. Phys. B85, 269 (1975).

10 D.H. Perkins, Vol. 4, p.214, XVI Int. Con. on H.E. Physics, Batavia, (1972).

11 S. Stein et al SLAC-PUB-1528 (1975)

12 R. McElhaney and S.F. Tuan, Phys. Rev. D8, 2267 (1973)

13 B. Barish; this conference.

14 B. Roe; this Conference

15 D. Cline, Proc. Palermo Conf. (1975)

16 E.G. Cazzoli et al Phys. Rev. Lett. 34, 1125 (1975).

17 L. Mo; this Conference

18 A. Benvenuti et al, Phys. Rev. Lett. 32, 125 (1974).

19 B. Aubert et al, Phys. Rev. Lett. 33, 984 (1974).

20 A. Benvenuti et al, Phys. Rev. Lett. 34, 419 (1975).

21 S.L. Adler, Phys. Rev. 143, 1144 (1966)

22 A. De Rujula, S. Georgi and S. Glashow, Phys. Rev. Lett. 35, 69 (1975).

23 M.R. Krishnaswamy et al, Phys. Lett. 57B, 105 (1975).

24 M.R. Krishnaswamy et al, Proc. Roy. Soc. A323, 489 (1971)

25 In his Palermo report[15], D. Cline first gives the form $(\pi/G^2)(d\sigma^{\nu n}/dq^2 - d\sigma^{\nu p}/dq^2) = 2$ for the Adler sumrule, and states that the form $(\pi/G^2)\,.\,(d\sigma^{\bar{\nu}p}/dq^2 - d\sigma^{\nu p}/dq^2) = 2$ or $(\pi/G^2)(d\sigma^{\bar{\nu}n}/dq^2 - d\sigma^{\nu n}/dq^2) = -2$ follows from charge symmetry and is therefore in doubt. The exact reverse is in fact the case. The ASR involves the isospin commutation relation $I_+I_- - I_-I_+ = I_+(I_+)^\dagger - I_-(I_-)^\dagger = 2I_3$ and therefore connects ν and $\bar{\nu}$ cross-sections for any hadron (p or n).

26 A. de Rujula, S. Georgi and S. Glashow, Phys. Rev. Lett. 35, 628, (1975)

27 Gargamelle beam-dump experiment; internal CERN/GGM report (Jan. 1972).

28 A. Benvenuti et al (HPWF collaboration) in the press.

29 It is to be noted that if a quasi-elastic cut $W^2 < 3$ GeV^2, is made to the HPWF data, the value of the difference $(d\sigma/dq^2 - d\bar{\sigma}/dq^2)$ is consistent with zero at all q^2. This is to be expected since, at the typical energies involved ($\sim$40 GeV), the V-A interference term for the quasi-elastic channels (proportional to $1/E$) will be small. This observed equality of the ν and $\bar{\nu}$ cross-sections at small W suggests that the anomaly observed (at larger W) is not simply due to the missing of events.